

Proceedings of the ASME 2018 International Mechanical Engineering Congress & Exposition
IMECE 2018
November 9–15, 2018, Pittsburgh, USA

IMECE2018-88543

ENTROPY GENERATION MINIMIZATION FOR ENERGY-EFFICIENT DESALINATION

John H. Lienhard V

Rohsenow Kendall Heat Transfer Laboratory
Department of Mechanical Engineering
Massachusetts Institute of Technology
Cambridge, MA 02139-4307 USA
email: lienhard@mit.edu

ABSTRACT

Desalination systems can be conceptualized as power cycles, in which the useful work output is the work of separation of fresh water from saline water. In this framing, thermodynamic analysis provides powerful tools for raising energy efficiency. This paper discusses the use of entropy generation minimization for a spectrum of desalination systems, including those based on reverse osmosis, humidification-dehumidification, membrane distillation, electrodialysis, and forward osmosis. The energy efficiency of desalination is shown to be maximized when entropy generation is minimized. Equipartition of entropy generation is considered and applied to these systems. The mechanisms of entropy generation in these systems are characterized, including the identification of major causes of irreversibility. Methods to limit discarded exergy are also identified. Prospects and technology development needs for further improvement are mentioned briefly.

NOMENCLATURE

A	Membrane permeability [$\text{mol m}^{-2} \text{bar}^{-1} \text{s}^{-1}$], or heat transfer area [m^2], by context
a_k	Activity of species k
c	Molar concentration [mol m^{-3}]
c_p	Specific heat capacity at constant pressure [$\text{J kg}^{-1} \text{K}^{-1}$]
\mathcal{D}	Diffusion coefficient [$\text{m}^2 \text{s}^{-1}$]
e_f	Flow exergy [J kg^{-1}]
\mathbf{E}	Electric field vector [V m^{-1}]
F	Faraday constant, 96485.333 [C mol^{-1}]

g	Specific Gibbs energy [J kg^{-1}]
\bar{g}_k	Molar Gibbs energy of pure solvent k [J mol^{-1}]
\dot{H}	Enthalpy flow rate [W]
h	Specific enthalpy [J kg^{-1}]
\bar{h}_k	Molar enthalpy of species k [J mol^{-1}]
h_{fg}	Latent heat of vaporization [J kg^{-1}]
\mathbf{J}_k	Flux vector of species k [$\text{mol m}^{-2} \text{s}^{-1}$]
\mathbf{J}_Q	Heat flux vector [W m^{-2}]
\mathbf{J}_U	Internal energy flux vector [W m^{-2}]
\mathbf{j}	Electric current density vector [A m^{-2}]
k	Thermal conductivity [$\text{W m}^{-1} \text{K}^{-1}$]
L_{ij}	Coupling coefficient matrix [units vary]
M_k	Molar mass of species k [g mol^{-1}]
\dot{m}	Mass flow rate [kg s^{-1}]
\mathcal{P}	Perimeter [m]
p	Hydraulic pressure [bar]
\dot{Q}	Heat transfer rate [W]
R	Universal gas constant, 8.31446 [$\text{J mol}^{-1} \text{K}^{-1}$]
r	Recovery ratio, \dot{m}_p/\dot{m}_{sw}
S	Entropy [J K^{-1}]
\dot{S}_{gen}	Entropy generation rate [W K^{-1}]
s	Specific entropy [$\text{J K}^{-1} \text{kg}^{-1}$]
\bar{s}_k	Molar entropy of species k [$\text{J K}^{-1} \text{mol}^{-1}$]
\dot{S}''_{gen}	Entropy generation rate per unit area [$\text{W m}^{-2} \text{K}^{-1}$]
T	Temperature [K]
U	Overall heat transfer coefficient [$\text{W m}^{-2} \text{K}^{-1}$]
\bar{v}_w	Molar volume of pure water [$\text{m}^3 \text{mol}^{-1}$]
\dot{W}	Work transfer rate [W]

\dot{W}_{least}	Least (reversible) work of separation ($r > 0$) [W]
$\dot{W}_{\text{least}}^{\text{min}}$	Minimum least work of separation ($r \rightarrow 0$) [W]
\dot{W}_{pump}	Pump work [W]
\dot{W}_{sep}	Work of separation [W]
w_k	Mass fraction of species k [g kg^{-1}]
\mathbf{X}_i	Driving force vector for flux [units vary]
x	Position coordinate, varies by context [m]
z_k	Valence of species k

Greek letters and symbols

Δ	Difference in a quantity, by context
ΔV_{cp}	ED cell pair voltage difference [V]
η_{II}	Second-law efficiency of desalination plant, Eqn. (10)
μ_k	Chemical potential of species k [J mol^{-1}]
Π_k	Osmotic pressure of species k [bar]
ρ	Mass density [g m^{-3}]
σ	Volumetric entropy generation rate [W m^{-3}]
∇_T	Constant temperature gradient, see Eqns. (15) and (16)

Subscripts

0	Restricted dead state
a	Air
b	Brine
c	Cold stream
H	High temperature heat source
h	Hot stream
in	Inlet state
k	Species k
p	Product
s	Salts
sw	Saline water (feed)
w	Water

Superscripts

*	Environment, or global, dead state
---	------------------------------------

Acronyms

ED	Electrodialysis
FO	Forward osmosis
GOR	Gained output ratio, Eqn. (32)
HCR	Modified heat capacity rate ratio, Eqn. (34)
HDH	Humidification-dehumidification
MD	Membrane distillation
RO	Reverse osmosis

INTRODUCTION

Desalination of seawater, brackish water, and wastewater has gained increasing importance in the face of rising population and changing climate [1]. As of June 2017, global desalination capacity exceeded 92 Mm³/day [2]. The energy efficiency of desalination plants has improved steadily over recent decades, but, for seawater desalination, energy still represents 30 to 40% of the cost of water. Today's state-of-the-art seawater reverse osmosis

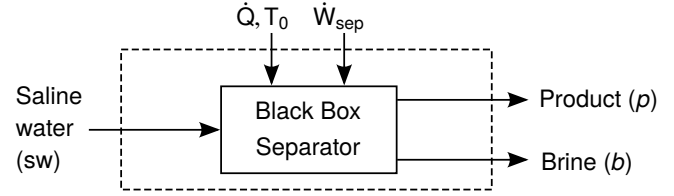


FIGURE 1. CONTROL VOLUME FOR A DESALINATION PLANT

plants require 3 to 4.5 kWh/m³ [3], of which 2 to 3 kWh/m² is consumed by the desalination process itself¹. The thermodynamic minimum energy for seawater desalination, at 50% water recovery, is just 1 kWh/m³. Consequently, considerable room for improvement remains.

Entropy generation minimization is a powerful and well-established tool for guiding energy efficiency improvements to a wide range of engineering systems, particularly power cycles. This paper describes the use of entropy generation minimization to improve desalination processes. Desalination plants are framed in the language of power cycles. Formulations based on Gibbs energy and flow exergy are shown, and the appropriate second-law efficiency is given. Entropy generation by transport processes is a special concern in desalination, which is a chemical separation process driven by mechanical work, heat transfer, or work done by electric fields. Entropy generation by these mechanisms is briefly reviewed and the role of equipartitioning is described. Then, the causes and reduction of entropy generation are discussed for several desalination processes, including systems based on reverse osmosis (RO), humidification-dehumidification (HDH), membrane distillation (MD), electrodialysis (ED), and forward osmosis (FO). Prospects for further improvement are identified.

DESALINATION AS A THERMAL POWER CYCLE

The basic operation of a desalination process is to separate a saline feed stream into a more pure *product* stream and a more saline *brine* stream (Fig. 1). Work is required to effect this separation, as provided, for example, by pumps in reverse osmosis desalination. Equivalently, heat transfer from a higher temperature source can also effect the separation, as in a variety of distillation processes.

The First and Second Laws of Thermodynamics may be applied to a control volume surrounding the desalination system in steady state:

$$\dot{W}_{\text{sep}} + \dot{Q} + (\dot{m}h)_{\text{sw}} = (\dot{m}h)_p + (\dot{m}h)_b \quad (1)$$

$$\frac{\dot{Q}}{T_0} + (\dot{m}s)_{\text{sw}} + \dot{S}_{\text{gen}} = (\dot{m}s)_p + (\dot{m}s)_b \quad (2)$$

¹All values are approximate and depend on various local considerations, including feed salinity, water recovery ratio, and plant characteristics.

In Eqns. (1) and (2), T_0 is the ambient temperature of the environment away from the system (to which heat is rejected), \dot{m}_i , h_i , and s_i are the mass flow rate, specific enthalpy and specific entropies of the saline water (sw), product (p), and brine (b) streams [4]. Heat and work are considered to be positive if they enter the system.

Elimination of \dot{Q} between these equations gives the work of separation

$$\dot{W}_{\text{sep}} = \dot{m}_p(h - T_0 s)_p + \dot{m}_b(h - T_0 s)_b - \dot{m}_{\text{sw}}(h - T_0 s)_{\text{sw}} + T_0 \dot{S}_{\text{gen}} \quad (3)$$

In the case that the entering and leaving streams are at the dead state pressure and temperature, T_0 and p_0 ,

$$\dot{W}_{\text{sep}} = \dot{m}_p g_p + \dot{m}_b g_b - \dot{m}_{\text{sw}} g_{\text{sw}} + T_0 \dot{S}_{\text{gen}} \quad (4)$$

where $g = h - T s$ is the specific Gibbs free energy².

The least work occurs for a reversible desalination plant, with $\dot{S}_{\text{gen}} = 0$:

$$\dot{W}_{\text{least}} = \dot{m}_p g_p + \dot{m}_b g_b - \dot{m}_{\text{sw}} g_{\text{sw}} \quad (5)$$

The least work is independent of the desalination process and depends only on the differences of Gibbs energy between the entering and leaving streams. For saline water, this means that the minimum least work will depend on the feed salinity, the pure water recovery ratio ($r = \dot{m}_p / \dot{m}_{\text{sw}}$), and, if the product is not essentially pure, the product water salinity. Least work is shown as a function of recovery ratio in Fig. 2 using the ionic composition of seawater at various concentrations (saline water properties are discussed in Appendix A). The minimum value of the least work, $\dot{W}_{\text{least}}^{\text{min}}$, occurs for infinitesimal recovery ratio ($r \rightarrow 0$) as if extracting just a small cup of pure water from an ocean of salty water.

If the leaving streams are at a temperature different from the dead state, exergy is being discarded as they exit, meaning that the work requirement will be greater than if they are at the dead state temperature. Streams leaving at pressures above the dead state also discard exergy, whereas as flow exergy below the dead state pressure is negative [6]. In addition, when the leaving streams are at the dead state temperature, the reversible system produces leaving streams of lower total entropy than the entering stream, and so heat must be rejected to the environment, according to Eqn. (2). If the system operates adiabatically ($\dot{Q} = 0$), the leaving streams have higher enthalpy (are warmer) than the entering stream, and the higher outlet temperature strongly raises

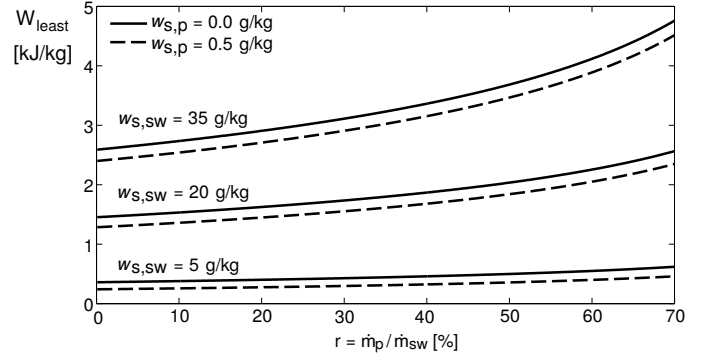


FIGURE 2. LEAST WORK OF SEPARATION VERSUS PURE WATER RECOVERY RATIO FOR VARIOUS FEED SALINITIES [5]. TYPICAL SEAWATER HAS A SALINITY OF 35 g/kg.

the outlet entropy for a given level of separation. Consequently, entropy usually must be generated, and the work requirement will be greater than if the streams exit at the dead state temperature.

Exergetic formulation

In the case that the outlet conditions are not at the dead state temperature and pressure Eqn. (3) may be recast in terms of the flow exergy function [5, 6]:

$$e_f = (h - h^*) - T_0 (s - s^*) + \sum_{k=1}^n w_k (\mu_k^* - \mu_{k,0}) / M_k \quad (6)$$

where a superscript * denotes that the temperature and pressure, but *not* the concentration, are at the environment condition (the restricted dead state); and subscript 0 denotes that temperature, pressure, and concentration are at the environment condition (the global dead state). Streams leaving a desalination plant are by design *not* at the environment's concentration. The result, using the fact that $\dot{m}_{\text{sw}} = \dot{m}_b + \dot{m}_p$, is

$$\dot{W}_{\text{sep}} = \dot{m}_p e_{f,p} + \dot{m}_b e_{f,b} - \dot{m}_{\text{sw}} e_{f,\text{sw}} + T_0 \dot{S}_{\text{gen}} \quad (7)$$

where the last term represents exergy destruction. In the case that the leaving streams are at the restricted dead state, Eqn. (7) reduces to Eqn. (4).

Distillation

If a desalination system operates by taking in a high temperature heat input, \dot{Q}_{sep} at T_H , as opposed to a work input, \dot{W}_{sep} , then some algebra shows that the work term in either Eqn. (4) or (7) may be replaced by the exergetically equivalent amount of

²An identical result is obtained if a control mass is considered rather than a control volume [5, footnote 7], although obviously without the dots above the symbols.

heat:

$$\dot{Q}_{\text{sep}} \left(1 - \frac{T_0}{T_H}\right) = \dot{W}_{\text{sep}} \quad (8)$$

As before, the plant may still reject heat to T_0 . Most distillation plants require both a heat and a work input (the latter being for liquid circulation pumps), so that a sum is needed on the lefthand side of the two equations mentioned, e.g.,

$$\dot{Q}_{\text{sep}} \left(1 - \frac{T_0}{T_H}\right) + \dot{W}_{\text{pump}} = \dot{m}_p e_{f,p} + \dot{m}_b e_{f,b} - \dot{m}_{\text{sw}} e_{f,\text{sw}} + T_0 \dot{S}_{\text{gen}} \quad (9)$$

Second-law efficiency

The second-law efficiency of a desalination plant, with respect to the exergy input that it receives, is [4, 5, 7, 8]

$$\eta_{II} = \frac{\dot{W}_{\text{least}}^{\text{min}}}{\dot{Q}_{\text{sep}} (1 - T_0/T_H) + \dot{W}_{\text{sep}} + \dot{W}_{\text{pump}}} \quad (10)$$

where \dot{W}_{sep} or \dot{Q}_{sep} and \dot{W}_{pump} may be zero depending upon the system in question. Equation (9) shows that η_{II} is maximized by minimizing the entropy generation and bringing the outlet streams toward the restricted dead state.

The second-law efficiency of a number of desalination plants at various feed salinities has been reported by Tow et al. [9]. Typical large seawater RO plants have a second-law efficiency in the range of 25 to 35%. For cases of combined water and power production, the second-law efficiency may instead be referred to primary energy [5, 7].

ENTROPY GENERATION BY TRANSPORT PROCESSES

Carrington and Sun and others [10, 11] have shown that the entropy generation per unit volume, σ , is given by

$$\sigma = \nabla \frac{1}{T} \cdot \mathbf{J}_U + \sum_k \left[\frac{z_k F \mathbf{E}}{T} - \nabla \left(\frac{\mu_k}{T} \right) \right] \cdot \mathbf{J}_k \quad (11)$$

where μ_k is the chemical potential per mole of species k , \mathbf{J}_k is the molar flux of k , \mathbf{E} is the electric field vector, F is Faraday's number, and z_k is the valence of k . The internal energy flux \mathbf{J}_U is related to the measurable heat flux \mathbf{J}_Q by

$$\mathbf{J}_U = \mathbf{J}_Q + \sum_k \bar{h}_k \mathbf{J}_k \quad (12)$$

where \bar{h}_k is the molar enthalpy of species k . The electric current density \mathbf{j} is

$$\mathbf{j} = F \sum_k z_k \mathbf{J}_k \quad (13)$$

With $\mu_k = \bar{h}_k - T \bar{s}_k$, for \bar{s}_k the molar entropy of species k ,

$$\sigma = \nabla \frac{1}{T} \cdot \mathbf{J}_Q + \frac{1}{T} \mathbf{E} \cdot \mathbf{j} + \nabla \frac{1}{T} \cdot \left(\sum_k \bar{h}_k \mathbf{J}_k \right) - \sum_k \nabla \left(\frac{\mu_k}{T} \right) \cdot \mathbf{J}_k \quad (14)$$

$$= \nabla \frac{1}{T} \cdot \mathbf{J}_Q + \frac{1}{T} \mathbf{E} \cdot \mathbf{j} - \frac{1}{T} \sum_k (\nabla \bar{h}_k - T \nabla \bar{s}_k) \cdot \mathbf{J}_k \quad (15)$$

The last two terms in the second equation are essentially the gradient of chemical potential evaluated at a constant temperature (i.e., by considering only its dependence on concentration and pressure), a point that has occasionally been overlooked. This gradient may be compactly denoted as ∇_T :

$$\sigma = \nabla \frac{1}{T} \cdot \mathbf{J}_Q + \frac{1}{T} \mathbf{E} \cdot \mathbf{j} - \frac{1}{T} \sum_k \nabla_T \mu_k \cdot \mathbf{J}_k \quad (16)$$

Terms accounting for viscous dissipation term and chemical reactions may be added to the entropy production if it is relevant to do so. For further discussion, see the lucid development in Kjelstrup et al. [11, Chap. 3, App. A].

ENTROPY GENERATION MINIMIZATION AND EQUIPARTITIONING

Equations (4), (7), and (9) show that the energy consumption of a desalination plant may be minimized by: *i*) minimizing entropy generation with respect to fixed conditions of water production, \dot{m}_p , and water recovery ratio, r ; and *ii*) bringing the outlet stream temperature and pressure closer to the restricted dead state, so as to avoid discarding useable exergy³. In view of the second consideration, pressure recovery devices (e.g., turbines or pressure exchangers) are essential components in reverse osmosis plants that produce an appreciable amount of high-pressure brine; and heat recuperation is essential the design of all distillation plants [13].

The first consideration leads to a need to minimize differences (or gradients) in temperature, concentration, or pressure

³If a lower salinity water source is available, chemical exergy can be recovered from the brine, e.g., by pressure-retarded osmosis (PRO). Blending the brine with additional feed water reduces entropy generation by up to $(\dot{W}_{\text{least}} - \dot{W}_{\text{least}}^{\text{min}})/T_0$ as the brine approaches the restricted dead state [4, §3.6]; however, the economics of PRO are challenging unless very large salinity differences are applied [12].

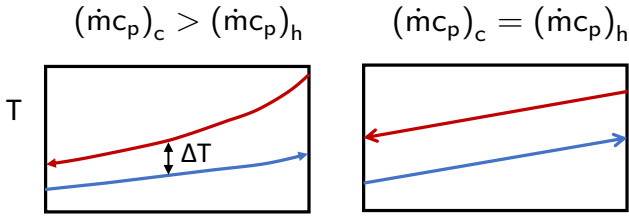
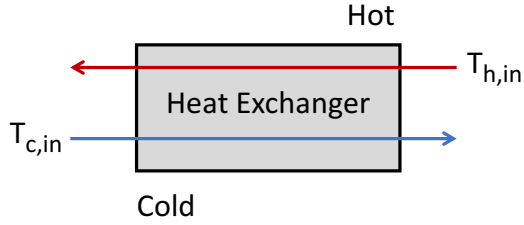


FIGURE 3. BALANCING A COUNTERFLOW HEAT EXCHANGER

throughout the system. Some straightforward ideas can be drawn from heat exchangers. Counterflow designs can transfer a given amount of heat between streams at different inlet temperatures while maintaining low local temperature differences. Further, balancing the heat capacity rates of the two streams [setting $(\dot{m}c_p)_h = (\dot{m}c_p)_c$] can make the local temperature difference between streams, ΔT , uniform over the length of the counterflow exchanger (Fig. 3). A balanced, counterflow heat exchanger has the minimum entropy generation for a given pair of inlet temperatures and heat exchanger effectiveness [14]. The concept of balanced counterflow has been extended to several desalination technologies, such as reverse osmosis, humidification-dehumidification, membrane distillation, and forward osmosis; and it has long been embedded in multistage flash and multi-effect desalination systems [13].

A balanced counterflow device having a given local ΔT can transfer a fixed amount of heat using less area, A , when the overall heat transfer coefficient, U , is larger. Alternatively, a larger U can facilitate a lower ΔT for a given area. Since the local entropy production of a small area $dA = \mathcal{P}dx$ is

$$d\dot{S}_{\text{gen}}'' = d\dot{Q} \left(\frac{1}{T_c} - \frac{1}{T_h} \right) \approx \frac{d\dot{Q} \Delta T}{T_c^2} = \frac{U\mathcal{P}\Delta T^2}{T_c^2} dx \quad (17)$$

integration (App. B) shows that the total entropy production is

$$\dot{S}_{\text{gen}} \approx \dot{Q} \left(\frac{\Delta T}{T_{h,\text{in}} T_{c,\text{in}}} \right) \quad (18)$$

At fixed UA , since $\dot{Q} = UA\Delta T$, a higher flux, more compact device generates the same entropy for a given heat load. On

the other hand, lowering ΔT (or in general, the pinch) can significantly lower entropy generation for a given \dot{Q} , which favors raising the product UA . Obviously, capital cost and fouling or maintenance considerations constrain all such choices. For example, if additional area is expensive and U cannot be raised, a higher ΔT may be necessary to limit capital investment, even though the greater irreversibility lowers energy efficiency.

Equipartitioning of Entropy Generation

Equation (16) has the form of a product of flux vectors \mathbf{J}_i and driving force vectors \mathbf{X}_i

$$\sigma = \sum_i \mathbf{X}_i \cdot \mathbf{J}_i \quad (19)$$

where the combinations can be seen by inspection⁴. Further, for many systems, the fluxes are an isotropic linear function of the driving forces⁵:

$$\mathbf{J}_i = \sum_j L_{ji} \mathbf{X}_j \quad (20)$$

Thus, σ is quadratic in the driving forces, e.g., proportional to square of temperature or concentration gradients:

$$\sigma = \sum_{i,j} \mathbf{X}_i L_{ji} \mathbf{X}_j \quad (21)$$

Tondeur and Kvaalen [17] considered systems of this type with a constant coupling matrix L_{ij} and operated at a fixed duty (amount of heat or mass to be transferred). They proved that reducing the spatial variance of the driving force (or the summed covariance for multiple forces) will minimize the overall entropy generation, assuming that the forces can be independently varied [18]. Indeed, that is exactly what is accomplished by balancing a counterflow heat exchanger to produce a uniform ΔT and minimize entropy production. Johannessen et al. [19] showed when the coupling matrix L_{ij} is not constant, entropy generation is minimized by minimizing the spatial variance of the entropy production itself. This minimization is referred to as equipartitioning of entropy generation.

In many cases (such as humidification) coupled driving forces (such as moist air temperature and humidity) cannot easily be varied independently [20]. Recent work by Magnanelli et al. [21] showed that even when forces cannot be fully separated,

⁴The pairings in Eqn. (16) are similar to, but not the same as, those in Eqn. (11). The relationship of driving forces to a fundamental equation for entropy is discussed by Callen [15] and Bejan [16], and various pairings are given in [11].

⁵For pure conduction $\mathbf{J}_Q = L_{QQ} \nabla(1/T) = -L_{QQ} T^{-2} \nabla T = -k \nabla T$.

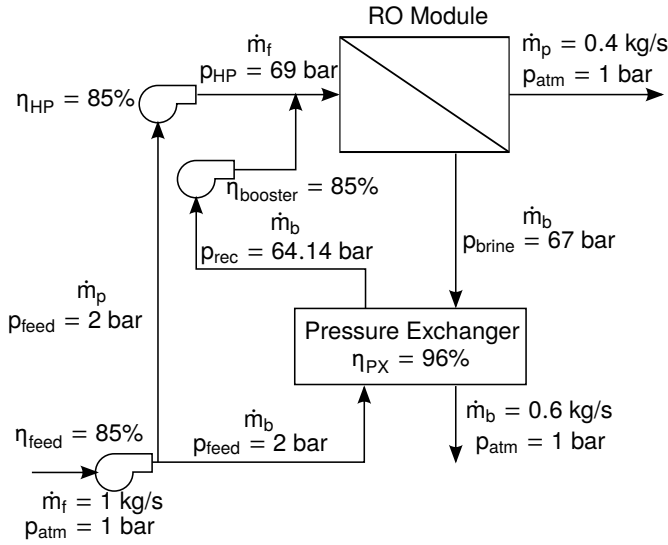


FIGURE 4. A SINGLE-STAGE REVERSE OSMOSIS SYSTEM [5]

the numerically optimal operating point is very close to that predicted by equipartitioning entropy production. Equipartitioning to increase the efficiency of desalination processes has been the subject of several studies [22–24], as will be discussed below.

REVERSE OSMOSIS

Reverse osmosis accounted for 65% of the world’s desalination capacity in 2015 [25]. RO is the dominant technology for brackish groundwater desalination and is rapidly displacing traditional thermal technologies for seawater desalination. The energy requirements for seawater RO were described in the introduction. For brackish water desalination, the pump pressures required are much lower (feeds have just 3 to 20% of seawater’s salinity); but cost optimization favors smaller, less energy-efficient systems that typically consume 0.3 to 1.5 kWh/m³ [26].

Various RO configurations are used depending on the condition of the saline feed water. We will focus on a basic single-stage seawater configuration (Fig. 4). Seawater enters at ambient pressure and is divided into two streams, one going directly to a high pressure pump and one entering a rotary pressure exchanger. Once both streams are brought to high pressure, they enter the RO membrane module. Low pressure fresh water and high pressure brine exit the module. The high pressure brine is sent to the pressure exchanger, which transfers its pressure to one of the feed streams. The brine exits the system at ambient pressure. The pressure exchanger is essential in recovering brine exergy after the RO module, bringing it close to the restricted dead state. Pressure recovery devices can lower energy consumption substantially and are universally applied in seawater systems, for which brine pressures are high and recovery ratios are limited.

In the RO module, the high pressure saline feed enters on one

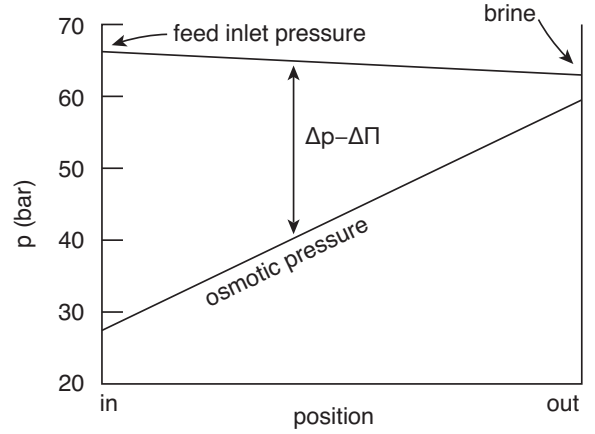


FIGURE 5. TYPICAL DISTRIBUTION OF FEED HYDRAULIC AND OSMOTIC PRESSURES IN A SEAWATER RO MODULE

side of a semi-permeable membrane and flows along the membrane. Water passes through the membrane, leaving most salts behind. As water is removed, the feed salinity rises, causing the osmotic pressure to rise over the length of the module. A typical distribution of hydraulic and osmotic pressure in a seawater RO module is shown in Fig. 5. The inlet hydraulic pressure must be high enough that the outlet (or brine) hydraulic pressure exceeds the outlet osmotic pressure, so that water can be forced through the membrane. Consequently, significantly more pressure is applied near the inlet than is necessary to produce water flux. The excess pressure generates substantial entropy: Mistry et al. showed that more than 50% of a representative RO system’s entropy generation occurs as a result of the pressure difference across the membranes [4]. This effect can be shown as follows.

The chemical potential of water in a saline solution is given by

$$\mu_w = \bar{g}_w + RT \ln(a_w) \quad (22)$$

where \bar{g}_w is the molar Gibbs energy of pure water, a_w is the activity of water in solution, and R is the universal gas constant. The effect of hydraulic pressure on Gibbs energy has essential importance. For the pure substance:

$$\frac{\partial \bar{g}_w}{\partial p} = \bar{v}_w \quad (23)$$

where \bar{v}_w is the molar volume of pure liquid water. The osmotic pressure of water in solution relative to pure water is

$$\Pi_w = -\frac{RT \ln(a_w)}{\bar{v}_w} \quad (24)$$

In this equation, the liquid is assumed to be incompressible so that the molar volume is independent of pressure.

To evaluate the entropy generation resulting from the transport of water through a membrane using Eqn. (16), $\nabla_T \mu_w$ is required:

$$\nabla_T \mu_w = \nabla_T (\bar{g}_w + RT \ln a_w) \quad (25)$$

$$= \bar{v}_w \nabla_T p - \bar{v}_w \nabla_T \Pi_w \quad (26)$$

$$= \bar{v}_w \nabla_T (p - \Pi_w) \quad (27)$$

With this result, integration of σ across the membrane thickness L gives the entropy generation per unit membrane area:

$$\dot{S}_{\text{gen}}'' = \int_0^L \sigma dx = \int_0^L \left[\nabla \frac{1}{T} \cdot \mathbf{J}_Q - \mathbf{J}_w \cdot \frac{\bar{v}_w}{T} \nabla_T (p - \Pi_w) \right] dx \quad (28)$$

$$= J_Q \left(\frac{1}{T_L} - \frac{1}{T_0} \right) + \frac{\bar{v}_w J_w}{T} (\Delta p - \Delta \Pi_w) \quad (29)$$

where Δ means feed value minus permeate value. The membrane's salt rejection is approximated to be 100%. The first term is the usual entropy production by heat transfer through a temperature difference; and for entire RO pressure vessels the temperature rise tends to be quite small (~ 0.5 K) [5] with unimportant heat fluxes, so this term is negligible. The water flux is expressed phenomenologically by the solution-diffusion model [27–29] as

$$J_w = A (\Delta p - \Delta \Pi_w) \quad (30)$$

where A is the membrane permeability in consistent units. Thus,

$$\dot{S}_{\text{gen}}'' = \frac{\bar{v}_w A}{T} (\Delta p - \Delta \Pi_w)^2 \quad (31)$$

The overpressurization seen near the inlet in Fig. 5 thus contributes greatly to the entropy generation and inefficiency of RO desalination. The standard configuration (Fig. 5) is far from equipartition [22]. Various different designs have been developed to counteract this effect, leading to better equipartitioning, including the following.

1. *Multistage RO*, in which two or more pumps are placed in series, so that the first stage operates at a lower pressure, removing some water from the feed. Later stages use higher hydraulic pressures to recover more water as the osmotic pressure becomes larger [30,31]. Multistage seawater plants have been demonstrated to save energy and achieve high water recovery ratios [31].

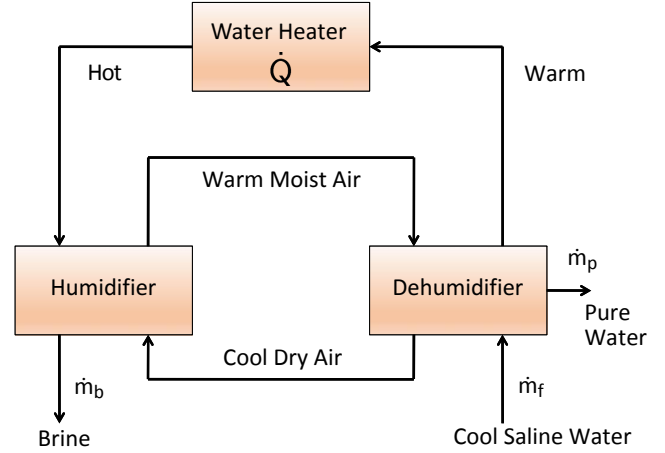


FIGURE 6. SCHEMATIC DRAWING OF A BASIC OPEN-AIR, CLOSED-WATER HDH SYSTEM.

2. *Batch RO*, in which a batch of saline feed is pressurized gradually as water is removed and the osmotic pressure rises [32,33]. Practical considerations limit the energy savings for seawater operation, but brackish water operation is more promising [34]. This technology is precommercial.
3. *Closed-cycle RO* is a semi-batch process that has been commercialized for brackish water desalination [35,36].
4. *Counterflow RO*, in which feed and permeate are counterflowing, so that osmotic pressure differences are kept low [37,38]. The reduced osmotic pressure difference reduces the hydraulic pressure and pump work required. This technology appears most promising for feeds at salinities greater than seawater. Commercial deployment is in progress.

Higher membrane permeability, A , is not effective in reducing energy consumption [39,40], but improved selectivity at low pressure may be [41].

HUMIDIFICATION-DEHUMIDIFICATION DESALINATION

Humidification-dehumidification desalination is used primarily for high salinity wastewater, as from oil/gas production, because its unit operations are highly tolerant of fouling. HDH transfers water vapor from a warm saline liquid feed into a carrier gas stream, usually air, which is then cooled to condense the water vapor as a pure liquid. A simplified HDH system is shown in Fig. 6. The dehumidifier is often a packed bed, with warm saline feed entering the top and cool air entering the bottom. State-of-the-art dehumidifiers use a multi-tray bubble column design, again with air and water in counterflow. The cycle in Fig. 6 is a simple open-water-loop, closed-air-loop arrangement; but current industrial systems use more complex configurations [42], often with an open air loop, a split closed water loop, and additional liquid-liquid heat exchangers for energy recovery.

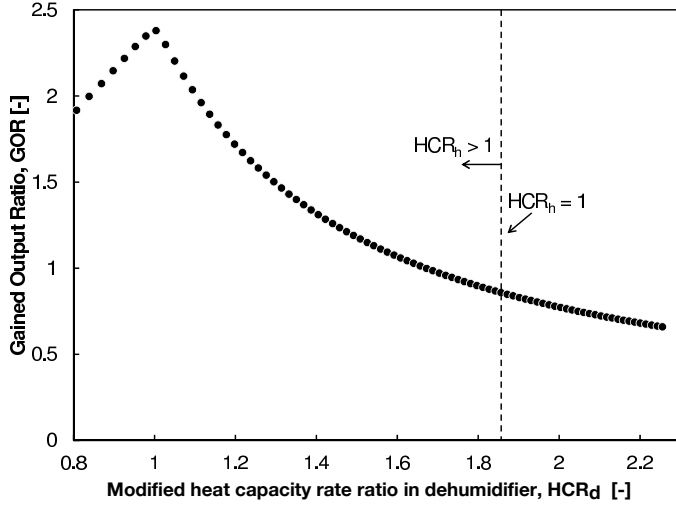


FIGURE 7. ENERGY EFFICIENCY (GOR) VERSUS HCR_d [23]

A principal design objective is to minimize the amount of heat, \dot{Q} , that must be provided by the water heater. The feed water is preheated in the dehumidifier by absorbing the latent of condensation. Thus, the dehumidifier recuperates some part of the energy transferred to the air stream by vaporization in the humidifier, helping to reduce \dot{Q} . Designing toward high effectiveness in these two heat and mass exchangers helps to limit the amount of exergy discarded with the leaving streams, also reducing \dot{Q} [43]. The energy (first-law) efficiency of HDH is usually characterized the gained-output-ratio, or GOR:

$$GOR = \frac{h_{fg}\dot{m}_p}{\dot{Q}} \quad (32)$$

which compares the latent heat required to vaporize the product water to the heat input. Well-designed experimental systems have reported GOR values as high as 2.6 for a single-stage system and up to 4.0 for a two-stage system [44].

The entropy production in HDH results primarily from heat and mass transfer in the gas phase. Thiel et al. [20] showed that Eqn. (16) can be reduced to

$$\sigma = k \left(\frac{\nabla T}{T} \right)^2 + \frac{\rho^2 R \mathcal{D}}{M_a M_w w_a w_w c} (\nabla w_w)^2 \quad (33)$$

indicating a strong influence of temperature and concentration gradients, where w_w is the water vapor mass fraction, \mathcal{D} is the diffusion coefficient, and other symbols are in the nomenclature list. Mistry et al. [45] showed that GOR for several HDH cycles was maximized as \dot{S}_{gen} was minimized. Numerical optimizations of cycles were subsequently reported by Mistry et al. [46].

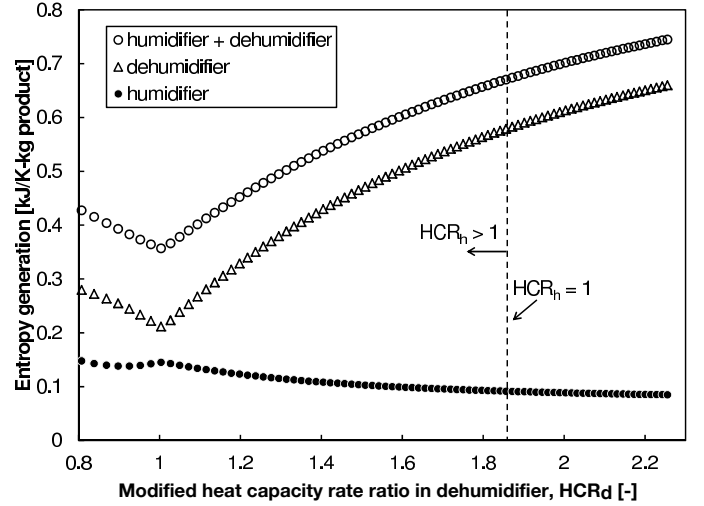


FIGURE 8. ENTROPY GENERATION VERSUS HCR_d [23]

Narayan et al. [14] showed that in simultaneous heat and mass exchangers of this class, entropy production can be minimized through balancing if a modified heat capacity rate ratio, HCR, is applied:

$$HCR = \frac{\Delta\dot{H}_{max, cold}}{\Delta\dot{H}_{max, hot}} \quad (34)$$

Here, $\Delta\dot{H}_{max}$ refers to the maximum possible change in the enthalpy rate of either counterflowing stream, e.g., as if an air stream is brought to saturation at the inlet temperature of an opposing water stream. This parameter can be computed from the inlet temperature, humidity, and mass flow rate of each stream.

Narayan et al. demonstrated that when the HCR of either component is equal to one, the entropy generation of that component is minimized. Chehayeb et al. [23] showed that the entropy production of the entire system is dominated by the dehumidifier (the shape of the saturation curve in the dehumidifier produces larger temperature differences between the air and water streams than in the humidifier), with the result that system performance is controlled by the HCR of the dehumidifier, HCR_d (Fig. 7). Further, Chehayeb et al. showed that entropy generation is minimized at the balanced condition, $HCR_d = 1$ (Fig. 8), as is the spatial variation of entropy production, indicating that the balanced condition is consistent with equipartitioning.

Multistage designs allow further opportunities for balancing by extracting air from the humidifier to the dehumidifier at an appropriate intermediate point [23, 47–49]. Industrial systems often use one such extraction. Significant interest has surrounded the potential to drive HDH systems with solar energy [50–52], although such designs have not been operated at large scale. Plate dehumidifiers have been considered [53, 54], but research around

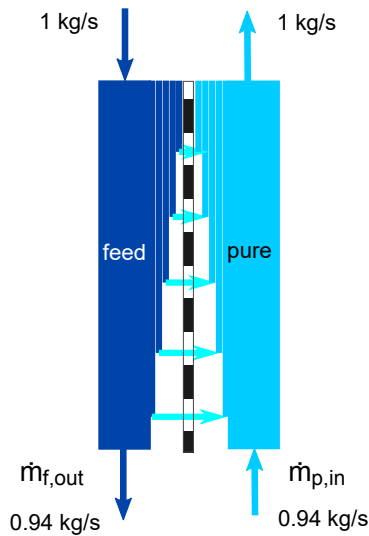


FIGURE 9. BALANCING DIRECT-CONTACT MEMBRANE DISTILLATION [63]

direct-contact components, especially bubble columns, has been most promising and has gone on to industrial use [55–61]. In particular, shallow bubble columns (similar to low-profile air strippers) can minimize hydrostatic pressure losses and blower power demand.

MEMBRANE DISTILLATION

Membrane distillation is an emerging technology that can operate on low-grade heat, such as solar thermal energy. A variety of designs have reached an early commercial stage, but deployment has been quite limited. Pilot-scale seawater MD systems have reported GOR values up to 7 ($90 \text{ kWh}_t/\text{m}^3$) with electrical consumption of $0.13 \text{ kWh}_e/\text{m}^3$ [62]. Research in this area is very active.

Membrane distillation is in many ways similar to HDH desalination, in that water is vaporized from a warm saline stream and condensed in a counterflow, heat recuperation arrangement [63–65]. However, in MD systems, the saline stream is separated from the fresh cooler stream by a hydrophobic, porous membrane through which vapor alone can pass. A variety of single-stage configurations have been proposed [66, 67], as well as multistage designs [68]. MD has the advantage of small vapor spaces, enabling compact equipment; but, as for other membrane processes, fouling is an important consideration [69].

Like HDH, the energy efficiency of MD systems can be improved by balancing appropriately defined heat capacity rates. In MD, purified liquid moves from the warm, saline stream to the opposing stream (Figs. 9 and 10). To define the proper capacity rates, the condensate must be taken into account [63–65]. For

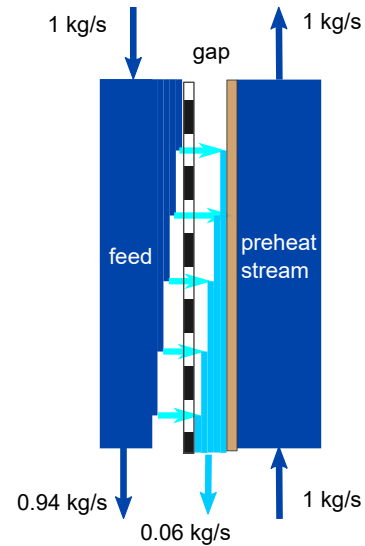


FIGURE 10. BALANCING AIR-GAP MEMBRANE DISTILLATION [63]

direct-contact MD, the condensate is incorporated into the cooler stream (Fig. 9), so that a balanced MD module would have the pure liquid entering at a lower mass flow rate than the saline stream inlet. For air-gap MD, the condensate is not added to the cooling stream; instead, its heat capacity rate is accounted for with that of the saline stream. In all cases, the effect of salinity on specific heat capacity must also be considered. A balanced direct-contact MD system can have a 50% higher GOR than an unbalanced one [65].

Further, as in HDH, minimization of temperature and concentration gradients between streams reduces the entropy production in MD. For a given configuration, raising the water flux through the membranes increases gradients and entropy production so that GOR falls, and vice versa. This behavior leads to a frequently reported GOR-flux trade-off, in which higher GOR can be achieved in MD systems lower flux [64, Fig. 3]. For a fixed water production, this trade-off shows that systems with larger membrane area will have greater energy efficiency, but at the expense of higher capital cost.

ELECTRODIALYSIS

Electrodialysis is primarily used for brackish groundwater desalination. For salinities below 2,000 ppm, ED has sometimes been reported to have significantly lower energy consumption than RO for representative designs [70], but this advantage is lost as salinity increases. ED is also used in Japan to concentrate seawater to a nearly saturated brine (200,000 ppm) for salt making [71, 72]. ED has seen renewed interest lately, with various new configurations nearing commercialization. For a 3,000 ppm feed, ED electrical energy consumption is roughly $0.8 \text{ kWh}/\text{m}^3$ [36].

Separation in electrodialysis results from an electric field imposed across alternating cation and anion exchange membranes. Chehayeb et al. have considered the entropy generation of ED [24, 73]. In this case, assuming locally isothermal conditions, Eqn. (16) has the form

$$\sigma = \frac{1}{T} \mathbf{E} \cdot \mathbf{j} - \frac{1}{T} \sum_k \nabla_T \mu_k \cdot \mathbf{J}_k \quad (35)$$

The distribution of entropy generation between the membranes and flow channels within an ED stack depends greatly on the salinity of the liquid streams. For high salinities, most entropy production results from ohmic resistance in the membranes, but at low salinities most occurs within the liquid channels [73]. The entropy generation of a cell pair per unit area can be approximated for a 1-1 electrolyte (e.g., NaCl) as [24, App. B]

$$\dot{S}_{\text{gen}}'' \approx \frac{j}{T} \left(\Delta V_{\text{cp}} - \frac{\Delta \mu_s}{F} \right) \quad (36)$$

where ΔV_{cp} is the voltage difference across a single cell pair and $\Delta \mu_s$ is the difference in chemical potential between the salt in the concentrate channel and that in the dilute channel⁶.

Chehayeb et al. [24] explored both counterflow and multi-staging of ED as means to achieve lower entropy generation by equipartitioning. They found that the high fixed costs of ED usually encourage small membrane areas that come with high average fluxes, so that the additional entropy generation associated with spatial imbalance does not contribute substantially to overall inefficiency. For those systems, equipartitioning provides little improvement in energy efficiency. However, if fixed costs can be lowered, so that greater membrane area is economically viable, multistaging could significantly reduce energy demand.

FORWARD OSMOSIS

Forward osmosis systems use osmotic pressure differences across a membrane to draw water from a saline feed stream that has undesirable characteristics (e.g., scalants or waste products) into a draw stream of higher osmotic pressure having a simpler or more desirable chemistry. A second process, such as RO or a thermal separation, then removes the water from the draw stream. Hydraulic pressure differentials between the feed and draw streams are usually negligible. FO has received significant attention in the past 15 years for its potential use in desalination, wastewater treatment, and pretreatment of feed water. Although FO seems unlikely to offer energetic advantages over direct desalination [74], its value in pretreatment and dewatering operations is

⁶This approximate result is also an example of how resistive losses and useful work appear together in entropy generation formulæ [11].

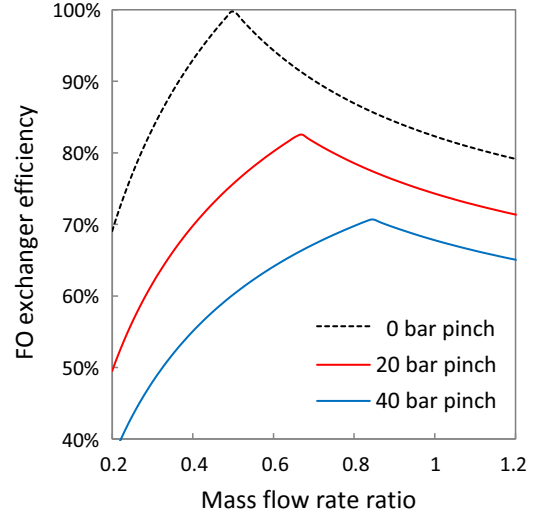


FIGURE 11. SECOND-LAW EFFICIENCY OF AN FO EXCHANGER VS. RATIO OF DRAW TO FEED MASS FLOW RATE FOR THREE VALUES OF THE PINCH PRESSURE DIFFERENCE [9]

well established [75]. FO appears to have reduced fouling compared to RO, although it is a misconception that this results from the lower hydraulic pressures of FO [76].

The FO exchanger can be evaluated separately from the water-recovery process that follows it. From Eqn. (31), the entropy generation per unit FO membrane area is

$$\dot{S}_{\text{gen}}'' = \frac{\bar{v}_w A}{T} (\Pi_{\text{draw}} - \Pi_{\text{feed}})^2 \quad (37)$$

Tow et al. [9] showed that the energy efficiency of forward osmosis exchangers could be improved by balancing the feed and draw stream mass flow rates so as to provide a uniform osmotic pressure difference between the counter-flowing streams. They provided analytical formulæ for the second-law efficiency as a function of mass flow rates and other parameters, identifying a particular mass flow-rate ratio that maximized efficiency for given feed and draw inlet salinities and water recovery ratio (Fig. 11).

SUMMARY

Entropy generation and discarded exergy in desalination systems directly raise the energy consumption of these increasingly important technologies. Desalination relies on mechanical, thermal, or electrical transport processes to separate pure water from saline water, and these transport processes dominate the entropy generation in desalination. By reducing gradients in temperature and concentration, and by making necessary gradients more spatially uniform, entropy generation can be minimized. System

designs that recover thermal energy or pressure work from leaving streams serve to reduce discarded exergy. Both approaches have guided substantial engineering improvements in the energy efficiency of desalination systems. Beyond the examples discussed here, these thermodynamic tools can reduce energy consumption in very demanding high salinity applications, including oil/gas produced water treatment [77] and zero-liquid discharge systems [78]. Continued emphasis on the thermodynamic aspects of system-level design are likely to result in further improvements and should be the focus of research on energy efficient desalination.

ACKNOWLEDGEMENT

I am grateful to Dr. Gregory P. Thiel for helpful comments on the manuscript.

REFERENCES

- [1] Schewe, J., et al., 2014. “Multimodel assessment of water scarcity under climate change”. *Proc. National Academy Sci.*, **111**(9), pp. 3245–3250. <http://www.pnas.org/content/111/9/3245>.
- [2] International Desalination Association, 2017. *IDA Desalination Yearbook 2017-2018*. Media Analytics, Oxford, UK.
- [3] Pankratz, T., 2017. “On the road to recovery”. *Water Desalination Report*, **53**(26), July.
- [4] Mistry, K. H., McGovern, R. K., Thiel, G. P., Summers, E. K., Zubair, S. M., and Lienhard, J. H., 2011. “Entropy generation analysis of desalination technologies”. *Entropy*, **13**(10), pp. 1829–1864. <http://www.mdpi.com/1099-4300/13/10/1829/>.
- [5] Lienhard, J. H., Mistry, K. H., Sharqawy, M. H., and Thiel, G. P., 2017. “Thermodynamics, exergy, and energy efficiency in desalination systems”. In *Desalination Sustainability: A Technical, Socioeconomic, and Environmental Approach*, H. A. Arafat, ed. Elsevier Publishing Co., Amsterdam, June, ch. 4. <https://dspace.mit.edu/handle/1721.1/109737>.
- [6] Sharqawy, M. H., Lienhard, J. H., and Zubair, S., 2011. “On exergy calculations for seawater with application to desalination systems”. *Intl. J. Thermal Sci.*, **50**(2), Feb., pp. 187–196. <http://doi.org/10.1016/j.ijthermalsci.2010.09.013>.
- [7] Mistry, K. H., and Lienhard, J. H., 2013. “Generalized least energy of separation for desalination and other chemical separation processes”. *Entropy*, **15**(6), pp. 2046–2080. <http://www.mdpi.com/1099-4300/15/6/2046>.
- [8] Warsinger, D. M., Mistry, K. H., Nayar, K. G., Chung, H. W., and Lienhard, J. H., 2015. “Entropy generation of desalination powered by variable temperature waste heat”. *Entropy*, **17**, Oct., pp. 7530–7566. <http://doi.org/10.3390/e17117530>.
- [9] Tow, E. W., McGovern, R. K., and Lienhard, J. H., 2015. “Raising forward osmosis brine concentration efficiency through flow rate optimization”. *Desalination*, **366**, pp. 71–79. <http://doi.org/10.1016/j.desal.2014.10.034>.
- [10] Carrington, C. G., and Sun, Z. F., 1991. “Second law analysis of combined heat and mass transfer phenomena”. *Intl. J. Heat Mass Transfer*, **34**(11), pp. 2767–2773. [https://doi.org/10.1016/0017-9310\(91\)90235-7](https://doi.org/10.1016/0017-9310(91)90235-7).
- [11] Kjelstrup, S., Bedeaux, D., Johannessen, E., and Gross, J., 2017. *Non-equilibrium thermodynamics for engineers*, 2nd ed. World Scientific Publishing Co., Singapore.
- [12] Chung, H. W., Banchik, L. D., Swaminathan, J., and Lienhard, J. H., 2017. “On the present and future economic viability of stand-alone pressure-retarded osmosis”. *Desalination*, **408**, pp. 133–144. <http://dx.doi.org/10.1016/j.desal.2017.01.001>.
- [13] El-Sayed, Y. M., and Silver, R. S., 1980. “Fundamentals of distillation”. In *Principles of Desalination*, K. S. Spiegler and A. D. Laird, eds., 2nd ed., Vol. A. Academic Press, New York, NY, ch. 2, pp. 55–109.
- [14] Narayan, G. P., Lienhard, J. H., and Zubair, S. M., 2010. “Entropy generation minimization of combined heat and mass transfer devices”. *Intl. J. Thermal Sci.*, **49**(10), Oct., pp. 2057–2066. <http://doi.org/10.1016/j.ijthermalsci.2010.04.024>.
- [15] Callen, H. B., 1985. *Thermodynamics and an Introduction to Thermostatistics*, 2nd ed. John Wiley & Sons, Inc.
- [16] Bejan, A., 1988. *Advanced Engineering Thermodynamics*. John Wiley & Sons, Inc.
- [17] Tondeur, D., and Kvaalen, E., 1987. “Equipartition of entropy production. An optimality criterion for transfer and separation processes”. *Ind. Eng. Chem. Res.*, pp. 50–56. <http://doi.org/10.1021/ie00061a010>.
- [18] Johannessen, E., and Kjelstrup, S., 2005. “A highway in state space for reactors with minimum entropy production”. *Chem. Eng. Sci.*, **60**, pp. 3347–3361. <http://doi.org/10.1016/j.ces.2005.01.026>.
- [19] Johannessen, E., Nummedal, L., and Kjelstrup, S., 2002. “Minimizing the entropy production in heat exchange”. *Intl. J. Heat Mass Transfer*, **45**(13), pp. 2649–2654. [http://doi.org/10.1016/S0017-9310\(01\)00362-3](http://doi.org/10.1016/S0017-9310(01)00362-3).
- [20] Thiel, G. P., and Lienhard, J. H., 2012. “Entropy generation in condensation in the presence of high concentrations of noncondensable gases”. *Intl. J. Heat Mass Transfer*, **55**, Sept., pp. 5133–5147. <http://doi.org/10.1016/j.ijthermalsci.2010.04.024>.
- [21] Magnanelli, E., Johannessen, E., and Kjelstrup, S., 2017. “Entropy production minimization as design principle for membrane systems: Comparing equipartition results to numerical optima”. *Ind. Eng. Chem. Res.*, **56**, April,

- pp. 4856–4866. <http://doi.org/10.1021/acs.iecr.7b00493>.
- [22] Thiel, G. P., McGovern, R. K., Zubair, S. M., and Lienhard, J. H., 2014. “Thermodynamic equipartition for increased second law efficiency”. *Applied Energy*, **118**, pp. 292–299. <http://doi.org/10.1016/j.apenergy.2013.12.033>.
- [23] Chehayeb, K. M., Narayan, G. P., Zubair, S. M., and Lienhard, J. H., 2015. “Thermodynamic balancing of a fixed-size two-stage humidification dehumidification desalination system”. *Desalination*, **369**, Aug., pp. 125–139. <http://doi.org/10.1016/j.desal.2015.04.021>.
- [24] Chehayeb, K. M., Nayar, K. G., and Lienhard, J. H., 2018. “On the merits of using multi-stage and counterflow electrodialysis for reduced energy consumption”. *Desalination*, **439**, Aug., pp. 1–16. <https://doi.org/10.1016/j.desal.2018.03.026>.
- [25] International Desalination Association, 2015. *IDA Desalination Yearbook 2015-2016*. Media Analytics, Oxford, UK.
- [26] Ahdab, Y., Thiel, G. P., Böhlke, J. K., Stanton, J., and Lienhard, J., 2018. “Minimum energy requirements for desalination of brackish groundwater in the united states”. *Water Research*, **141**, Sept., pp. 387–404. <https://doi.org/10.1016/j.watres.2018.04.015>.
- [27] Spiegler, K. S., and Kedem, O., 1966. “Thermodynamics of hyperfiltration (reverse osmosis): criteria for efficient membranes”. *Desalination*, **1**, pp. 311–326. [https://doi.org/10.1016/S0011-9164\(00\)80018-1](https://doi.org/10.1016/S0011-9164(00)80018-1).
- [28] Wijmans, J., and Baker, R., 1995. “The solution-diffusion model: a review”. *J. Membrane Sci.*, **107**, pp. 1–21. [https://doi.org/10.1016/0376-7388\(95\)00102-1](https://doi.org/10.1016/0376-7388(95)00102-1).
- [29] Paul, D., 2004. “Reformulation of the solution-diffusion theory of reverse osmosis”. *J. Membrane Sci.*, **241**(2), pp. 371–386. <https://doi.org/10.1016/j.memsci.2004.05.026>.
- [30] Wei, Q. J., McGovern, R. K., and Lienhard, J. H., 2017. “Saving energy with an optimized two-stage reverse osmosis system”. *Environ. Sci.: Water Res. Technol.*, **3**, pp. 659–670. <http://dx.doi.org/10.1039/C7EW00069C>.
- [31] Kurihara, M., Yamamura, H., and Nakanishi, T., 1999. “High recovery/high pressure membranes for brine conversion SWRO process development and its performance data”. *Desalination*, **125**, Nov., pp. 9–15. [http://doi.org/10.1016/S0011-9164\(99\)00119-8](http://doi.org/10.1016/S0011-9164(99)00119-8).
- [32] Warsinger, D. M., Tow, E. W., Nayar, K. G., Maswadeh, L. A., and Lienhard, J. H., 2016. “Energy efficiency of batch and semi-batch CCRO reverse osmosis desalination”. *Water Research*, **106**, pp. 272–282. <https://doi.org/10.1016/j.watres.2016.09.029>.
- [33] Swaminathan, J., Stover, R. L., Tow, E. W., Warsinger, D. M., and Lienhard, J. H., 2017. “Effect of practical losses on optimal design of batch RO systems”. In Proceedings of IDA World Congress on Desalination and Water Reuse, Sao Paulo, Brazil, International Desalination Association, pp. IDA17WC–58334. <http://hdl.handle.net/1721.1/111971>.
- [34] Swaminathan, J., Tow, E. W., Stover, R. L., and Lienhard, J. H., 2018. “Practical aspects of batch ro design for energy-efficient seawater desalination”. Under review.
- [35] Stover, R. L., 2013. “Industrial and brackish water treatment with closed circuit reverse osmosis”. *Desalin. Water Treat.*, pp. 1124–1130. <https://doi.org/10.1080/19443994.2012.699341>.
- [36] Nayar, K. G., Wright, N. C., Thiel, G. P., Winter, A. G., and Lienhard, J. H., 2015. “Energy requirements of alternative technologies for desalinating groundwater for irrigation”. In IDA World Congress on Desalination and Water Reuse. Paper No. IDAWC15–Nayar-b.
- [37] Bartholomew, T. V., Mey, L., Arena, J. T., Siefert, N. S., and Mauter, M. S., 2017. “Osmotically assisted reverse osmosis for high salinity brine treatment”. *Desalination*, **421**, pp. 3–11. <https://doi.org/10.1016/j.desal.2017.04.012>.
- [38] Bouma, A. T., and Lienhard, J. H., 2018. “Split-feed counterflow reverse osmosis for brine concentration”. Under review.
- [39] McGovern, R. K., and Lienhard, J. H., 2016. “On the asymptotic flux of ultrapermeable seawater reverse osmosis membranes due to concentration polarisation”. *J. Membrane Sci.*, **520**, Dec., pp. 560–565. <http://doi.org/10.1016/j.memsci.2016.07.028>.
- [40] Cohen-Tanugi, D., McGovern, R. K., Dave, S., Lienhard, J. H., and Grossman, J. C., 2014. “Quantifying the potential of ultra-permeable desalination membranes”. *Energy Environ. Sci.*, **7**(3), Feb., pp. 1134–1141. <http://doi.org/10.1039/C3EE43221A>.
- [41] Kurihara, M., Sasaki, T., Nakatsuji, K., Kimura, M., and Henmi, M., 2015. “Low pressure SWRO membrane for desalination in the Mega-ton Water System”. *Desalination*, **368**, pp. 135–139. <https://doi.org/10.1016/j.desal.2015.02.037>.
- [42] Lienhard, J. H., 2018. “Humidification-dehumidification desalination”. In *Desalination: Water from Water*, J. Nocera, ed., 2nd ed. Wiley-Scrivener, Salem, MA.
- [43] Narayan, G. P., Mistry, K. H., Sharqawy, M. H., Zubair, S. M., and Lienhard, J. H., 2010. “Energy effectiveness of simultaneous heat and mass exchange devices”. *Front. Heat Mass Transfer*, **1**(2), Aug., pp. 1–13. <http://doi.org/10.5098/hmt.v1.2.3001>.
- [44] Narayan, G. P., St. John, M., Zubair, S. M., and Lienhard, J. H., 2013. “Thermal design of the humidification dehumidification desalination system: an experimental investigation”. *Intl. J. Heat Mass Transfer*, **58**(3), March, pp. 740–748. <https://doi.org/10.1016/j.ijheatmasstransfer.2012.11.035>.
- [45] Mistry, K. H., Lienhard, J. H., and Zubair, S. M., 2010. “Effect of entropy generation on the performance of

- humidification-dehumidification desalination cycles”. *Intl. J. Thermal Sci.*, **49**(9), Sept., pp. 1837–1847. <http://doi.org/10.1016/j.ijthermalsci.2010.05.002>.
- [46] Mistry, K. H., Mitsos, A. H., and Lienhard, J. H., 2011. “Optimal operating conditions and configurations for humidification-dehumidification desalination cycles”. *Intl. J. Thermal Sci.*, **50**(5), May, pp. 779–789. <http://doi.org/10.1016/j.ijthermalsci.2010.12.013>.
- [47] McGovern, R. K., Thiel, G. P., Narayan, G. P., Zubair, S. M., and Lienhard, J. H., 2013. “Performance limits of single and dual stage humidification dehumidification desalination systems”. *Applied Energy*, **102**, Feb., pp. 1081–1090. <http://doi.org/10.1016/j.apenergy.2012.06.025>.
- [48] Chehayeb, K. M., Narayan, G. P., Zubair, S. M., and Lienhard, J. H., 2014. “Use of multiple extractions and injections to thermodynamically balance the humidification dehumidification desalination system”. *Intl. J. Heat Mass Transfer*, **68**, Jan., pp. 422–434. <http://doi.org/10.1016/j.ijheatmasstransfer.2013.09.025>.
- [49] Narayan, G. P., Chehayeb, K. M., McGovern, R. K., Thiel, G. P., Zubair, S. M., and Lienhard, J. H., 2013. “Thermodynamic balancing of the humidification dehumidification desalination system by mass extraction and injection”. *Intl. J. Heat Mass Transfer*, **57**(2), Feb., pp. 756–770. <http://doi.org/10.1016/j.ijheatmasstransfer.2012.10.068>.
- [50] Summers, E. K., Antar, M. A., and Lienhard, J. H., 2012. “Design and optimization of an air heating solar collector with integrated phase change material energy storage for use in humidification-dehumidification desalination”. *Solar Energy*, **86**(11), Nov., pp. 3417–3429. <http://doi.org/10.1016/j.solener.2012.07.017>.
- [51] Summers, E. K., Lienhard, J. H., and Zubair, S. M., 2011. “Air-heating solar collectors for humidification-dehumidification desalination systems”. *J. Solar Energy Engineering*, **113**(1), Feb., p. 011016. <http://doi.org/10.1115/1.4003295>.
- [52] Summers, E. K., Lienhard, J. H., and Zubair, S. M., 2010. “Air-heating solar collectors for humidification-dehumidification desalination systems”. In Proc. 14th Intl. Heat Transfer Conference. Washington DC.
- [53] Sievers, M., and Lienhard, J. H., 2013. “Design of flat-plate dehumidifiers for humidification dehumidification desalination systems”. *Heat Transfer Eng.*, **34**(7), Jan., pp. 543–561. <http://doi.org/10.1080/01457632.2013.730355>.
- [54] Sievers, M., and Lienhard, J. H., 2015. “Design of plate-fin tube dehumidifiers for humidification-dehumidification desalination systems”. *Heat Transfer Eng.*, **36**(3), Feb., pp. 223–243. <http://doi.org/10.1080/01457632.2014.916153>.
- [55] Narayan, G. P., Sharqawy, M. H., Lam, S., Das, S. K., and Lienhard, J. H., 2013. “Bubble columns for condensation at high concentrations of noncondensable gas: Heat transfer model and experiments”. *AIChE J.*, **59**(5), pp. 1780–1790. <https://doi.org/10.1002/aic.13944>.
- [56] Tow, E. W., and Lienhard, J. H., 2013. “Analytical modeling of a bubble column dehumidifier”. In Proc. ASME 2013 Summer Heat Transfer Conf. Paper No. HT2013-17763. <http://dx.doi.org/10.1115/HT2013-17763>.
- [57] Tow, E. W., and Lienhard, J. H., 2014. “Measurements of heat transfer coefficients to cylinders in shallow bubble columns”. In Proc. 15th Intl. Heat Transfer Conference, IHTC-15. Paper No. IHTC15-8857, http://web.mit.edu/lienhard/www/papers/conf/IHTC15-8857_Tow.pdf.
- [58] Tow, E. W., and Lienhard, J. H., 2014. “Heat transfer to a horizontal cylinder in a shallow bubble column”. *Intl. J. Heat Mass Transfer*, **79**, pp. 353 – 361. <https://doi.org/10.1016/j.ijheatmasstransfer.2014.08.021>.
- [59] Tow, E. W., and Lienhard, J. H., 2014. “Experiments and modeling of bubble column dehumidifier performance”. *Intl. J. Thermal Sci.*, **80**, pp. 65–75. <https://doi.org/10.1016/j.ijthermalsci.2014.01.018>.
- [60] Narayan, G. P., Lam, S., and St. John, M., 2017. Systems including a condensing apparatus such as a bubble column condenser. US Patent #9700811.
- [61] Liu, H., and Sharqawy, M. H., 2016. “Experimental performance of bubble column humidifier and dehumidifier under varying pressure”. *Intl. J. Heat Mass Transfer*, **93**, pp. 934–944. <https://doi.org/10.1016/j.ijheatmasstransfer.2015.10.040>.
- [62] Duong, H. C., Cooper, P., Nelemans, B., Cath, T. Y., and Nghiem, L. D., 2016. “Evaluating energy consumption of air gap membrane distillation for seawater desalination at pilot scale level”. *Sep. Purif. Technol.*, **166**, pp. 55–62. <https://doi.org/10.1016/j.seppur.2016.04.014>.
- [63] Swaminathan, J., Chung, H. W., Warsinger, D. M., and Lienhard, J. H., 2018. “Energy efficiency of membrane distillation up to high salinity: Evaluating critical system size and optimal membrane thickness”. *Applied Energy*, **211**, pp. 715–734. <https://doi.org/10.1016/j.apenergy.2017.11.043>.
- [64] Swaminathan, J., Chung, H. W., Warsinger, D. M., and Lienhard, J. H., 2016. “Membrane distillation model based on heat exchanger theory and configuration comparison”. *Applied Energy*, **184**, pp. 491–505. <http://doi.org/10.1016/j.apenergy.2016.09.090>.
- [65] Swaminathan, J., Chung, H. W., Warsinger, D. M., and Lienhard, J. H., 2016. “Simple method for balancing direct contact membrane distillation”. *Desalination*, **383**, April, pp. 53–59. <http://doi.org/10.1016/j.desal.2016.01.014>.
- [66] Summers, E. K., Arafat, H. A., and Lienhard, J. H., 2012. “Energy efficiency comparison of single stage membrane distillation (MD) desalination cycles in different configurations”. *Desalination*, **290**, pp. 54–66. <http://doi.org/10.1016/j.desal.2012.01.004>.

- [67] Swaminathan, J., Chung, H. W., Warsinger, D., Al-Marzooqi, F., Arafat, H. A., and Lienhard, J. H., 2016. “Energy efficiency of permeate gap and novel conductive gap membrane distillation”. *J. Membrane Sci.*, **502**, pp. 171–178. <http://doi.org/10.1016/j.memsci.2015.12.017>.
- [68] Chung, H. W., Swaminathan, J., Warsinger, D. M., and Lienhard, J. H., 2016. “Multistage vacuum membrane distillation (MSVMD) systems for high salinity applications”. *J. Membrane Sci.*, **497**, pp. 128–141. <https://doi.org/10.1016/j.memsci.2015.09.009>.
- [69] Warsinger, D. M., Swaminathan, J., Guillen-Burrieza, E., Arafat, H. A., and Lienhard, J. H., 2015. “Scaling and fouling in membrane distillation for desalination applications: A review”. *Desalination*, **356**, Jan., pp. 294–313. <http://dx.doi.org/10.1016/j.desal.2014.06.031>.
- [70] Wright, N. C., and Winter, A. G., 2014. “Justification for community-scale photovoltaic-powered electro dialysis desalination systems for inland rural villages in india”. *Desalination*, **352**, pp. 82–91. <https://doi.org/10.1016/j.desal.2014.07.035>.
- [71] Strathmann, H., 2004. *Ion-exchange membrane separation processes*. Elsevier B. V., Amsterdam.
- [72] Nayar, K. G., Fernandes, J., McGovern, R. K., McCance, A., Al-Anzi, B. S., and Lienhard, J. H., 2018. “Cost and energy requirements of hybrid RO and ED systems for salt production”. *Desalination*. Under review.
- [73] Chehayeb, K. M., and Lienhard, J. H., 2017. “Entropy generation analysis of electro dialysis”. *Desalination*, **413**, July, pp. 184–198. <http://doi.org/10.1016/j.desal.2017.03.001>.
- [74] McGovern, R. K., and Lienhard, J. H., 2014. “On the potential of forward osmosis to energetically outperform reverse osmosis desalination”. *J. Membrane Sci.*, **469**, pp. 245–250. <https://doi.org/10.1016/j.memsci.2014.05.061>.
- [75] Johnson, D. J., Suwaileh, W. A., Mohammed, A. W., and Hilal, N., 2018. “Osmotic’s potential: An overview of draw solutes for forward osmosis”. *Desalination*, **434**, pp. 100 – 120. <https://doi.org/10.1016/j.desal.2017.09.017>.
- [76] Tow, E. W., and Lienhard, J. H., 2017. “Unpacking compaction: Effect of hydraulic pressure on alginate fouling”. *J. Membrane Sci.*, **544**, pp. 221 – 233. <https://doi.org/10.1016/j.memsci.2017.09.010>.
- [77] Thiel, G. P., Tow, E. W., Banchik, L. D., Chung, H. W., and Lienhard, J. H., 2015. “Energy consumption in desalinating produced water from shale oil and gas extraction”. *Desalination*, **366**, pp. 94–112. <http://doi.org/10.1016/j.desal.2014.12.038>.
- [78] Chung, H. W., Nayar, K. G., Swaminathan, J., Chehayeb, K. M., and Lienhard, J., 2017. “Thermodynamic analysis of brine management methods: zero-discharge desalination and salinity-gradient power production”. *Desalination*, **404**, Feb., pp. 291–303. <http://doi.org/10.1016/j.desal.2016.11.022>.
- [79] Nayar, K. G., Sharqawy, M. H., Banchik, L. D., and Lienhard, J. H., 2016. “Thermophysical properties of seawater: A review and new correlations that include pressure dependence”. *Desalination*, **387**, July, pp. 1–24. <http://doi.org/10.1016/j.desal.2016.02.024>. Codes available at <http://web.mit.edu/seawater>.
- [80] Sharqawy, M. H., Lienhard, J. H., and Zubair, S. M., 2010. “Thermophysical properties of seawater: A review of existing correlations and data”. *Desal. Water Treat.*, **16**, pp. 354–380. <http://doi.org/10.5004/dwt.2010.1079>. Codes available at <http://web.mit.edu/seawater>.
- [81] Nayar, K. G., Panchanathan, D., McKinley, G. H., and Lienhard, J., 2014. “Surface tension of seawater”. *J. Phys. Chem. Ref. Data*, **43**(4), Nov., p. 43103. <http://doi.org/10.1063/1.4899037>.
- [82] Thiel, G. P., and Lienhard, J. H., 2014. “Treating produced water from hydraulic fracturing: composition effects on scale formation and desalination system selection”. *Desalination*, **346**, pp. 54–69. <http://doi.org/10.1016/j.desal.2014.05.001>.
- [83] Mistry, K. H., and Lienhard, J. H., 2013. “Effect of nonideal solution behavior on desalination of a sodium chloride solution and comparison to seawater”. *J. Energy Resour. Technol.*, **135**(4), p. 042003. <https://doi.org/10.1115/1.4024544>.
- [84] Mistry, K. H., Hunter, H. A., and Lienhard, J. H., 2013. “Effect of composition and nonideal solution behavior on desalination calculations for mixed electrolyte solutions with comparison to seawater”. *Desalination*, **318**, pp. 34–47. <https://doi.org/10.1016/j.desal.2013.03.015>.

APPENDIX A: THERMOPHYSICAL PROPERTIES OF SALINE WATER

The thermophysical properties of saline water differ from pure water, particularly the specific heat capacity, density, and vapor pressure. For seawater, the ionic composition is relatively uniform around the world, and extensive data sets and software libraries are available [79–81]. For brackish groundwater, the ionic composition varies significantly with location [26]; and for produced water (from drilling operations), the salinities can be far higher than seawater with highly variable compositions [82]. Both groundwater and seawater properties can be simulated using the Pitzer-Kim model [82]. Sodium chloride solution is sometimes used for simplified calculations [83, 84], but its properties differ somewhat from naturally occurring saline waters, especially in the absence of insoluble, scale-forming components.

APPENDIX B: ENTROPY GENERATION IN A BALANCED COUNTERFLOW HEAT EXCHANGER

For a balanced counterflow exchanger of length L , $T_c = T_{c,in} + ax$ where the constant $a = (T_{c,out} - T_{c,in}) / L$. Integrating eqn. (17) for $\Delta T \ll T_{c,out}$ gives eqn. (18):

$$\dot{S}_{\text{gen}} = U\mathcal{P}\Delta T^2 \int_0^L \frac{dx}{(T_{c,in} + ax)^2} \quad (38)$$

$$= \frac{U\mathcal{P}\Delta T^2}{a} \left(\frac{1}{T_{c,in}} - \frac{1}{T_{c,out}} \right) \quad (39)$$

$$= \left(\frac{\dot{Q}\Delta T}{T_{c,in}T_{c,out}} \right) \quad (40)$$

$$\approx \left(\frac{\dot{Q}\Delta T}{T_{c,in}T_{h,in}} \right) \quad (18)$$